

Pushing and Pulling Ponderomotive Forces in Wavepackets and Beat Waves

Yury Bliokh

Physics Department, Technion—Israel Institute of Technology, Haifa 320003, Israel

We consider ponderomotive forces acting on small particles in propagating wave packets (pulses). Specifically, we analyze simple point particles as well as composite dipole and dumbbell particles in the fields of forward-propagating (parallel phase and group velocities) and backward-propagating (antiparallel phase and group velocities) wave packets. Depending on the characteristics of the wave packet, particles may be pushed away from the wave source or pulled toward it. We also examine particle dynamics in the field of a beat wave generated by two forward-propagating waves with slightly different frequencies. Such a beat wave can emulate a periodic sequence of either forward- or backward-propagating pulses. In particular, this provides a simple mechanism for realizing pulling forces as employed in optical and acoustic ‘tractor beams’.

I. INTRODUCTION

Ponderomotive forces determine the time-averaged motion of a particle in a fast-oscillating field of arbitrary nature. This concept is usually associated with the dynamics of particles in wave fields, but the first example is provided by a mechanical phenomenon: stabilization of the inverted pendulum by high-frequency vertical vibrations of its pivot: the so-called Kapitsa pendulum [1]. Later, gradient ponderomotive forces have been employed for trapping of charged particles in an inhomogeneous oscillating electromagnetic field [2].

Nowadays, ponderomotive forces on particles in inhomogeneous wave fields of different natures are widely explored in various scientific domains. This includes laser-driven plasma-based accelerators of charged particles, as well as optical and acoustic manipulation of neutral particles ranging from individual atoms to macroscopic biological samples, see reviews [3–8].

Most optical and acoustic studies on wave-induced forces imply monochromatic fields

(such as focused laser beams or standing ultrasonic waves) with inhomogeneous but stationary intensity distributions. At the same time, propagating wave packets (pulses) provide another fundamental class of wave fields, where spatial and temporal inhomogeneities act coherently. Surprisingly, the peculiarities of ponderomotive forces and particle dynamics in propagating wave packets have not been systematically analyzed (apart from the specific problem of wake-field acceleration of charged particles in plasma [5, 9]).

In this work, we examine the generic problem of 1D small-particle dynamics in propagating wavepacket fields. We explore the cases of point and composite particles, as well as wave packets with parallel and antiparallel phase and group velocities. Our study focuses on the pushing or pulling action of the ponderomotive force with respect to the wave source. Time-varying propagating fields have been shown as one of promising mechanisms for the ‘tractor-beam’ pulling action [10–12].

II. SIMPLE POINT PARTICLES

We consider a point particle in the 1D field of a quasi-monochromatic wave packet with a slowly varying amplitude: $a(x, t) \sin(\omega t - kx)$, where k is the central wavenumber and ω is the central wave frequency. Introducing dimensionless coordinate of the particle, $\xi = |k|x$, and dimensionless time $\tau = \omega t$, the non-relativistic equation of motion of the particle can be written as

$$\frac{d^2\xi}{d\tau^2} = \mathcal{F}(\xi, \tau) = a(\xi, \tau) \sin(\tau - s\xi). \quad (1)$$

Here \mathcal{F} is the force, $s = \text{sgn}(k)$, and we omit inessential constant factors. For a propagating wave packet, $a(\xi, \tau) = a(\xi - \eta_g \tau)$, where η_g is the dimensionless group velocity of the wave. In the follows, we assume that $\eta_g > 0$. In turn, the wave number k can be either positive or negative, i.e., the wave phase velocity can be parallel ($s = 1$) or antiparallel ($s = -1$) to the group velocity. Waves with parallel and antiparallel phase and group velocities will be referred to as the *forward* and *backward* waves, respectively.

Let the wave amplitude is small, $a \ll 1$, and slowly (adiabatically) varying function, $|da/d\xi| \ll a$ and $|da/d\tau| \ll a$. Then, using the perturbation approach, the solution of Eq. (1) can be presented as the sum of fast-oscillating, $\tilde{\xi}(\tau)$, and slow-varying, $\bar{\xi}(\tau)$, functions: $\xi(\tau) = \tilde{\xi}(\tau) + \bar{\xi}(\tau)$. In the first-order approximation in a and $da/d\tau$, Eq. (1) yields the

oscillating component:

$$\tilde{\xi} = -a \sin(\tau - s\bar{\xi}) - 2 \frac{\partial a}{\partial \tau} \cos(\tau - s\bar{\xi}). \quad (2)$$

Substituting $\xi(\tau) = \tilde{\xi}(\tau) + \bar{\xi}(\tau)$ in Eq. (1) and expanding the right-hand side into the Taylor series, with subsequent averaging over the oscillation period, results in equation for the slow-varying component:

$$\frac{d^2 \bar{\xi}}{d\tau^2} = -\frac{1}{4} \left(\frac{\partial a^2}{\partial \bar{\xi}} - 2s \frac{\partial a^2}{\partial \tau} \right) \equiv \mathcal{F}_{\text{pond}}, \quad (3)$$

where $\mathcal{F}_{\text{pond}}$ is the ponderomotive force acting on the particle.

Expression (3) shows that the ponderomotive force depends on the both spatial and temporal variations of the wave amplitude, where the corresponding contributions can be associated with the ‘gradient force’ [2] and the ‘wave-momentum’ force, respectively [13]. Since in a propagating wave packet, the spatial and temporal gradients of the amplitude are interconnected, these two forces act together. Substituting $a(\xi, \tau) = a(\xi - \eta_g \tau)$ into Eq. (3), the ponderomotive force takes the form

$$\mathcal{F}_{\text{pond}} = -\frac{1}{4} (1 + 2s\eta_g) \frac{da^2}{d\bar{\theta}}, \quad (4)$$

where $\bar{\theta} = \bar{\xi} - \eta_g \tau$.

Hereafter, until Section IV, we assume that the wave amplitude $a(\xi, \tau)$ has the form of an isolated propagating pulse, e.g., of a Gaussian form:

$$a(\theta) = a_0 \exp(-\theta^2/2\mathcal{L}_p^2), \quad (5)$$

where $\mathcal{L}_p \gg 1$ is the dimensionless pulse length.

The usual gradient force [the first term in Eq. (3)] is directed oppositely to the amplitude gradient. This is also true for the wavepacket-induced force (4), when the group and phase velocities are co-directed, $s = 1$. The situation changes if the group and phase velocities are antiparallel, $s = -1$. Depending on the value of the dimensionless group velocity η_g (i.e., actually the ratio of the dimensional group velocity $v_g = d\omega/dk$ to the phase velocity $v_{\text{ph}} = \omega/k$), the particle can be either repelled ($\eta_g < 1/2$) or attracted ($\eta_g > 1/2$) by the maximum-amplitude region.

Since the force (4) is proportional to the total derivative of the squared amplitude, it is conservative. Therefore, the particle, which was motionless before the pulse came, remains

motionless after the pulse passes, but it changes its position. When the group and phase velocities are co-directed, the particle is always shifted along the pulse propagation direction. In contrast, a wave packet with antiparallel group and phase velocities shifts the particle forward or backward, or even leaves the particle position unchanged, depending on the value of the group velocity η_g . This result is confirmed by numerical solution of Eqs. (1) and (3), and presented in Fig. 1.

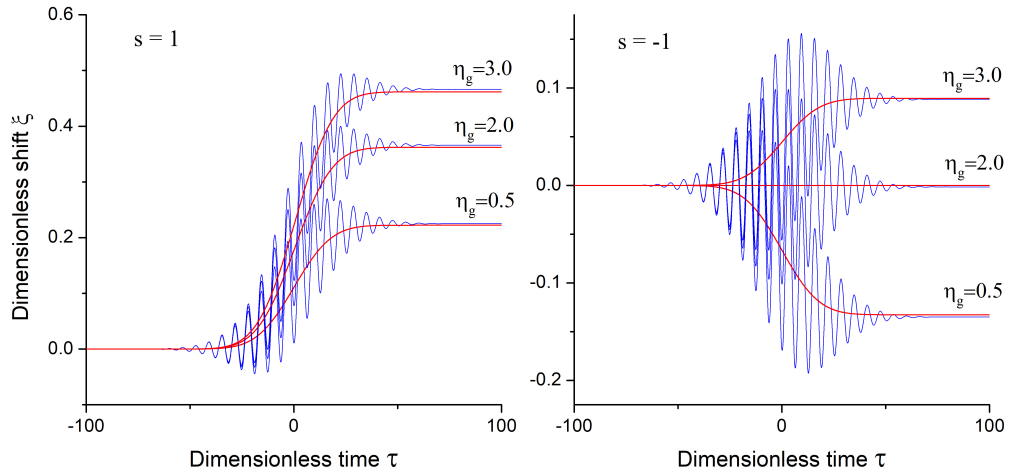


Figure 1. Longitudinal shift of the particle under the action of the pulses with different relations $\eta_g = v_g/v_{ph}$ between the wave phase, v_{ph} , and group, v_g , velocities. Thin oscillating lines – solution of Eq. (1), thick smooth lines – solution of Eq. (3). (a)– the phase and group velocities are co-directed, $s = 1$. (b)– the phase and group velocities are anti-parallel, $s = -1$.

III. COMPOSITE PARTICLES

We now consider simple models of composite particles consisting of two point particles connected by a massless rod. Namely, we examine three cases:

- (i) Two particles of the same “charge” (i.e., response to the acting wave field) connected by a rigid rod, such that this *dumbbell* can move along the x -axis and change its orientation with respect to it. This can model particles of anisotropic shapes, such as spheroids [14].
- (ii) Similar composite particle but with opposite “charges” of two point particles. This model corresponds to a *permanent dipole*, such as molecules with an intrinsic electric-dipole moment [15].
- (iii) Induced dipole particles, for which the dipole moment (the rod length) is proportional

to the applied wave field. Such particles are ubiquitous for optical and acoustic systems [16, 17].

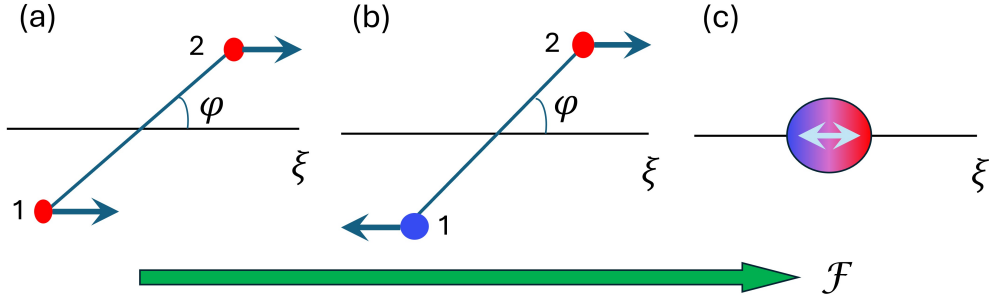


Figure 2. Composite particle. Two sub-particles of: (a) – equal (dumbbell, $\sigma = 1$), (b) – opposite (dipole, $\sigma = -1$) “charges” are connected by the massless rod of length d . (c) – induced dipole (polarizable) particle, whose dipole moment (the rod length) is proportional to the applied field.

The composite particles in the cases (i) and (ii) possess an additional rotational degree of freedom, and their motion is described by the position of the center of mass, ξ , and the angle φ between the rod and the x -axis, see Fig. 2. This brings about the equations of motion for the translational and rotational degrees of freedom:

$$\frac{d^2\xi}{d\tau^2} = \frac{1}{2} \left[\sigma \mathcal{F} \left(\xi - \frac{d}{2} \cos \varphi \right) + \mathcal{F} \left(\xi + \frac{d}{2} \cos \varphi \right) \right], \quad (6)$$

$$\frac{d^2\varphi}{d\tau^2} = \frac{d}{2I} \sin \varphi \left[\sigma \mathcal{F} \left(\xi - \frac{d}{2} \cos \varphi \right) - \mathcal{F} \left(\xi + \frac{d}{2} \cos \varphi \right) \right]. \quad (7)$$

Here, d is the dimensionless distance between the two point particles, $I = d^2/2$ is the corresponding moment of inertia of the composite particle, $\sigma = 1$ for the dumbbell model (i), and $\sigma = -1$ for the permanent dipole model (ii). For the induced dipole case (iii), $\sigma = -1$, it is always aligned with the force, so that $\varphi \equiv 0$, and the distance between the point particles is proportional to the wave-induced force, $d = \alpha \mathcal{F}$ (α is the polarizability coefficient).

Equations (6) and (7) can be simplified if the distance between point particles is small compared to the wavelength, $d \ll 1$ (the Rayleigh-particle limit):

$$\frac{d^2\xi}{d\tau^2} \simeq \frac{1}{2} \left[(1 + \sigma) \mathcal{F} + \frac{d}{2} (1 - \sigma) \cos \varphi \mathcal{F}' \right], \quad (8)$$

$$\frac{d^2\varphi}{d\tau^2} \simeq \frac{1}{d} \sin \varphi \left[(\sigma - 1) \mathcal{F} - \frac{d}{2} (1 + \sigma) \cos \varphi \mathcal{F}' \right]. \quad (9)$$

where

$$\mathcal{F}' \equiv \frac{d\mathcal{F}}{d\xi} = \frac{da}{d\theta} \sin(\tau - s\xi) - sa(\theta) \cos(\tau - s\xi) \simeq -sa(\theta) \cos(\tau - s\xi) \quad (10)$$

Equations (8)–(10) contain only the leading terms. The role of the discarded terms $\propto d^2$ and $\propto da/d\theta$ will be discussed below.

A. Dumbbell

We first consider the case of a dumbbell particle. The motion of the center of mass in the wave packet field is described by Eq. (8) with $\sigma = 1$, which coincides with the equation of motion (1) of a point particle and can be considered separately from Eq. (9). This results in the time-averaged evolution described by Eqs. (3) and (4). The time-averaged motion of the angle φ can be obtained in a similar way:

$$\frac{d^2\bar{\varphi}}{d\tau^2} = -\frac{1}{4}a^2(\bar{\theta}) \sin 2\bar{\varphi} (1 + \cos 2\bar{\varphi}). \quad (11)$$

Examples of the numerical solutions of the approximate time-averaged Eqs. (3) and (11) and exact Eqs. (6) and (7) are shown in Fig. 3.

Variations of the argument $\bar{\theta} = \bar{\xi} - \eta_g\tau$ along the dumbbell trajectory are induced mainly by the time τ (the particle shift $\bar{\xi}$ is small). Therefore, the amplitude a in Eq. (11) can be considered as a function of time only. Introducing a new time variable $\tau_* = \int_0^\tau d\tau' a(\tau')$, which varies from 0 to some finite value τ_*^{\max} , one can present Eq. (11) as follows:

$$\frac{d^2\bar{\varphi}}{d\tau_*^2} + \frac{1}{a} \frac{da}{d\tau_*} \frac{d\bar{\varphi}}{d\tau_*} = -\frac{d\mathcal{U}}{d\bar{\varphi}}, \quad (12)$$

where $\mathcal{U} = -1/4 \cos^4 \bar{\varphi}$ is the ponderomotive potential for the rotational degree of freedom. The second term on the left-hand side of Eq. (12) can be neglected when the wave packet duration τ_p is large enough: $a_0\tau_p \gg 1$. Then, Eq. (12) becomes the equation of motion of a point particle in the potential well \mathcal{U} . Its solution describes *slow* oscillations of the averaged angle $\bar{\varphi}$. The substitution $\tau \rightarrow \tau_*$ deforms the time scale, but does not change the amplitude of these oscillations, which remains approximately constant inside the wave packet, as shown in Fig. 3(b). After the wave packet passes, the particle remains rotating with a constant angular velocity $d\bar{\varphi}/d\tau$.

Thus, the initially motionless dumbbell acquires rotational motion, and, hence, some energy from the wave packet. However, the wave packet cannot transfer energy without

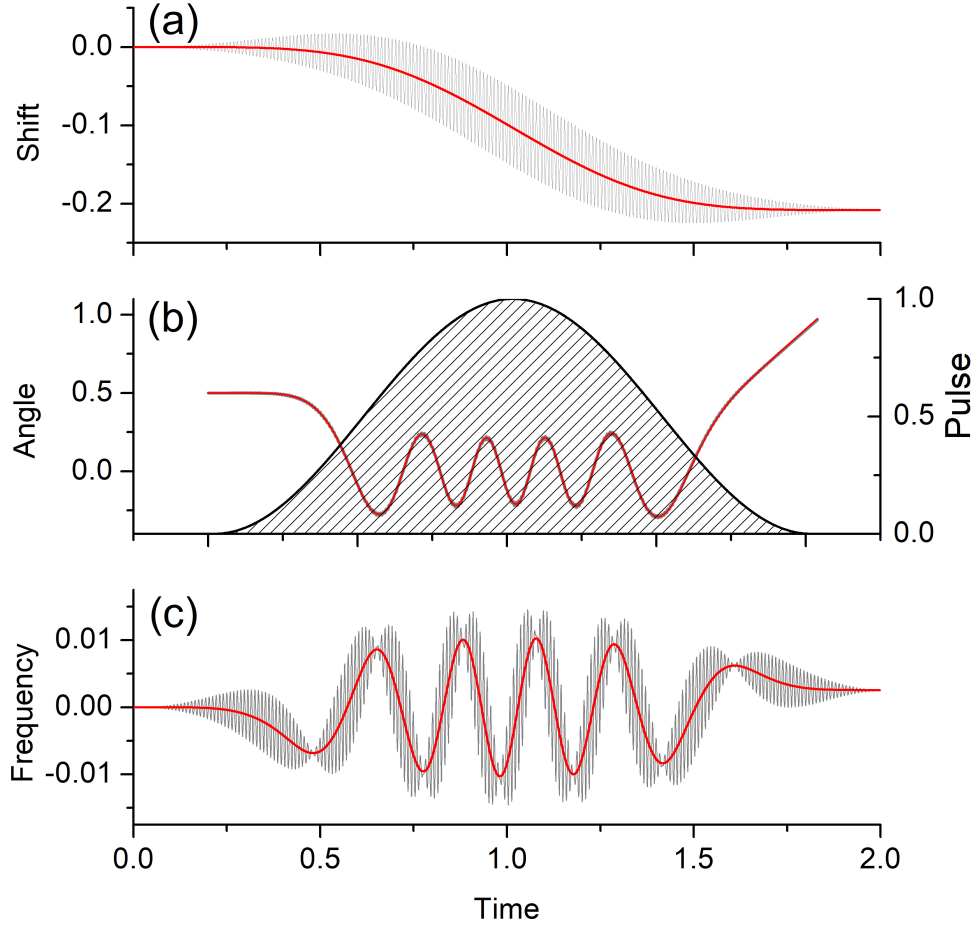


Figure 3. Evolution of the dumbbell center of mass (a), the rotation angle (b), and frequency $\nu = d\varphi/d\tau$ under the action of the backward wave ($s = -1$) pulse. Parameters of the pulse are: $a_0 = 0.05$, $\eta_g = 0.75$. The dumbbell rod length $d = 0.1$. Gray lines – solutions of complete equation Eq. (6) and (7); red lines – solutions of time-averaged equations Eq. (3) and (11); shaded area – pulse shape. Time is normalized to the pulse duration $\tau_p = \theta_0/\eta_g$.

linear momentum. Therefore, the particle must also gain some linear momentum, and, unlike the point particle, the final dumbbell's velocity $d\xi/d\tau$ must differ from its initial velocity. This is inconsistent with the conservative character of the gradient force in Eqs. (3) and (4) for the translational motion. This controversy originates from the terms neglected in the transition from Eqs. (6), (7) to the simplified Eqs. (8)–(10) and (3), (4); it will be analysed

in Section III C.

B. Permanent dipole

Let us now consider the motion of a permanent dipole particle, case (ii), described by Eqs. (8) and (9) with $\sigma = -1$. Since $d \ll 1$, the right-hand side of Eq. (8) is much less than the right-hand side of Eq. (9). Therefore, here we neglect the change in the center-of-mass position ξ , and consider only the dynamics of the rotation angle φ :

$$\frac{d^2\varphi}{d\tau^2} = -\frac{2}{d} \sin \varphi a(\theta) \sin(\tau - s\xi) \Big|_{\xi=\text{const}}. \quad (13)$$

(The slow motion of the center of mass will be considered in the next subsection.) Representing the angle as the sum of fast-oscillating and slow-varying parts, $\varphi = \tilde{\varphi} + \bar{\varphi}$, we derive the time-averaged equation of motion:

$$\frac{d^2\bar{\varphi}}{d\tau^2} = -\frac{a^2}{d^2} \sin 2\bar{\varphi}. \quad (14)$$

Notably, this equation coincides with the equation of motion of the *Kapitsa pendulum* in the absence of gravitation field [18]. Namely, it describes oscillations near the equilibrium positions $\bar{\varphi} = 0$ and $\bar{\varphi} = \pi$ in the ponderomotive potential well $\mathcal{U} = a^2/d^2 \sin^2 \bar{\varphi}$. Therefore, the angular motion of a permanent dipole is qualitatively similar to the dumbbell case (i). The essential quantitative difference is that the condition $a_0 \ll 1$, which allows the separation of the fast and slow motions, is now replaced by a stronger condition $a_0 \ll d \ll 1$, which can be violated even when the pulse amplitude is small.

Figure 4 shows numerical solutions of exact Eqs. (6) and (7) for 50 dipoles, whose initial orientation angles $\varphi(0)$ are randomly distributed over the interval $(0, \pi)$. When $a_0/d \ll 1$, the angles oscillate near the equilibrium points $\varphi = 0$ and $\varphi = \pi$ (Fig. 4a), in agreement with the approximate Eq. (14). As the small parameter a_0/d increases, the oscillation frequency increases but the amplitude is not affected much. Furthermore, a fraction of the dipoles leave the equilibrium regime of finite angular oscillations, and starts to *rotate* rapidly, and can even occasionally change the rotation direction (Fig. 4b). The number of such rotating dipoles increases with the pulse amplitude, and for $a_0/d \sim 1$ the angular motion becomes chaotic (Fig. 4c), as described for the Kapitsa pendulum [19, 20].

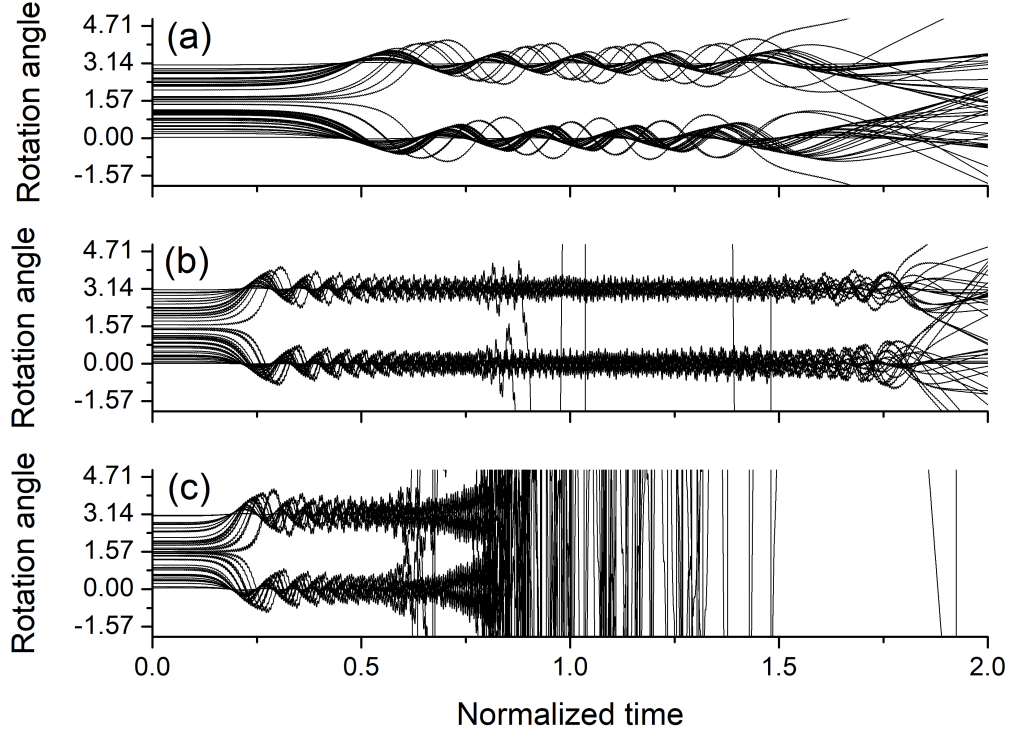


Figure 4. The angular oscillations of 50 dipoles, whose initial rotation angles $\varphi(0)$ are randomly distributed over the interval $(0, \pi)$. (a) – $a_0 = 0.002$; (b) – $a_0 = 0.02$; (c) – $a_0 = 0.03$. The oscillation frequency increases with increased wave amplitude, while the oscillation amplitude remains practically unchanged.

C. Energy and momentum transfer

As we discussed in Section III A, rotation of a composite particle after the wave packet passes implies that the wave energy and momentum are partially transferred to the particle. From energy and momentum conservation laws, it follows that the ratio of the kinetic energy (\mathcal{W}) and 1D momentum (\mathcal{P}) of the particle must be equal to the ratio of the frequency and wavevector in the wave, i.e., in the dimensionless variables, $\mathcal{P}/\mathcal{W} = s = \pm 1$ [21].

To verify this result, we numerically solved the exact Eqs. (8) and (9) for 500 composite particles, initially motionless and randomly oriented, $\varphi(0) \in (-\pi, \pi)$. We considered both forward ($s = 1$) and backward ($s = -1$) wave packets with various group-velocity parameters η_g , as well as both dumbbell ($\sigma = 1$) and permanent-dipole ($\sigma = -1$) particles. After the wave packet passes, the composite particle acquires final momentum $\mathcal{P} = 2d\xi/d\tau$ and kinetic energy $\mathcal{W} = \mathcal{P}^2/4 + I(d\varphi/d\tau)^2/2$, whose values are plotted in Fig. 5. One can see that these

quantities satisfy the relation $\mathcal{P}/\mathcal{W} = s$ with a very good accuracy.

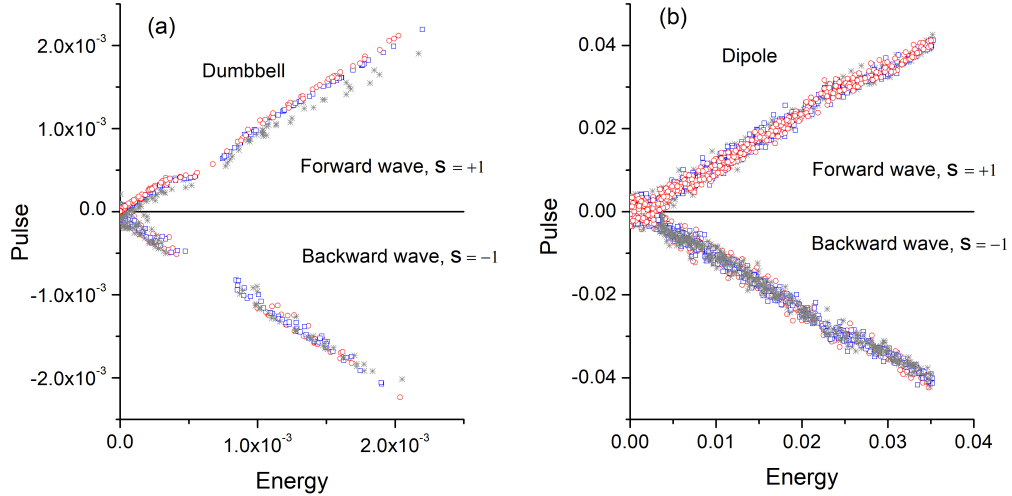


Figure 5. The relation between the energy and the momentum of composite particles after the pulse passage. Open circles, open squares, and stars mark results related to the parameter η_g values 0.5, 1.0, and 2.0, respectively.

D. Induced dipole

We now consider case (iii) of a *polarizable* particle with induced dipole moment. The dynamics of such a particle in a 1D wave packet is described by a single translational degree of freedom ξ , which obeys Eq. (8) with $\sigma = -1$ and $d = \alpha\mathcal{F}$:

$$\frac{d^2\xi}{d\tau^2} = \alpha\mathcal{F} \frac{d\mathcal{F}}{d\xi}. \quad (15)$$

This equation has quadratic right-hand side, and its straightforward averaging over fast wave oscillations yields

$$\frac{d^2\bar{\xi}}{d\tau^2} = \frac{\alpha}{4} \frac{da^2}{d\bar{\xi}} \equiv \mathcal{F}_{\text{pond}}. \quad (16)$$

This is a well-known gradient force that underpins optical or acoustic trapping of small particles [7]. It is conservative and has a form similar to that for a simple particle, Eqs. (3) and (4). After the wave packet passes, the initially motionless particle remains motionless, but its position is shifted towards or backwards the wave-packet source depending on the sign of the polarizability α and independently of the sign of the phase velocity, s .

IV. BEAT WAVES

In this Section, we examine potential applications of the ponderomotive forces in wavepacket-like fields to transport particles. Since a conservative gradient force induced by a single wavepacket shifts the particle, a suitable set of wave pulses can transport the particle over an arbitrary distance. Note that in contrast to a steady-force motion, which appears in monochromatic fields, here the particle experiences a stepwise motion. It is particularly appealing to be able to control the transport direction using forward and backward wavepackets, similar to “optical conveyors” and “tractor beams” [10, 22, 23].

Remarkably, particle manipulation by backward wave pulses has not been systematically explored so far. Backward electromagnetic waves with anti-parallel phase and group velocities ($s = -1$) appear in the so-called double-negative (or left-handed) media [24], which are characterized by simultaneously negative permittivity $\epsilon < 0$ and permeability $\mu < 0$, and are usually realized by complex periodic lattices composed of metal and dielectric elements [25]. There are also waveguides that support modes with negative phase velocity and have a free channel for electron beam transport [26, 27]. In addition, there are surface backward waves propagating along an interface between two media, such as plasma-vacuum interface [28]. In principle, particle manipulation can be realized in such structures, but the presence of unavoidable material elements makes this challenging.

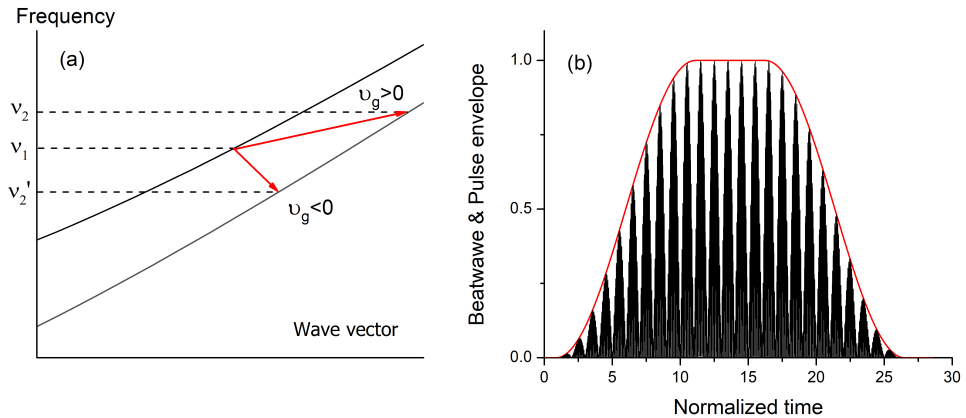


Figure 6. (a) – The dispersion characteristics $\nu(\kappa)$ of two modes of a waveguide. Depending on the relation between the frequencies ν_1 and ν_2 (ν'_2), the beat wave has either positive or negative effective group velocity u_g . (b) – The pulse envelope a (red line) and the beat wave sub-pulses (black line). Time is normalized to the beat wave period $2\pi/\Delta\nu$.

Notably, there is another, much simpler method to control the effective direction of the wavepacket propagation, which mimics backward waves but does *not* require anti-parallel phase and group velocities. Namely, we consider a *beat wave*, which is produced by the interference of two modes with close frequencies and wavevectors:

$$\mathcal{F}(\xi, \tau) = a_1 \cos(\kappa_1 \xi - \nu_1 \tau) - a_2 \cos(\kappa_2 \xi - \nu_2 \tau). \quad (17)$$

Here, the dimensionless frequencies $\nu_{1,2} = 1 \pm \Delta\nu$ and wavevectors $\kappa_{1,2} = 1 \pm \Delta\kappa$ of the two waves obey different dispersion relations, such as, e.g., $\nu_{1,2}^2 = \kappa_{1,2}^2 + \nu_{c1,2}^2$ for two modes of a waveguide with cut-off frequencies $\nu_{c1,2}$, see Fig. 6a. The field (17) with $a_1 = a_2 \equiv a/2$, $|\Delta\nu| \ll 1$, $|\Delta\kappa| \ll 1$ can be written as:

$$\mathcal{F}(\xi, \tau) = a \sin(\xi - \tau) \sin(\Delta\kappa \xi - \Delta\nu \tau), \quad (18)$$

This field has a form of a traveling wave $\propto \sin(\xi - \tau)$ with periodic slowly varying amplitude $a \sin(\Delta\kappa \xi - \Delta\nu \tau)$, i.e., it mimics a *periodic sequence of wavepackets* (hereafter, referred to as *sub-pulses*). Here, the wave phase velocity $u_{\text{ph}} = 1$ is always positive, whereas the effective group velocity (i.e., the direction of motion) of sub-pulses $u_g = \Delta\nu/\Delta\kappa$ can be either positive or negative. (Note that the wave energy flow is always forward-directed.) Thus, one can control the motion of sub-pulses forward or backward to the wave source by varying the wave frequencies (Fig. 6a).

One can expect that the motions of a particle in a set of isolated wavepackets and in the beat wave (18) are similar. There is a significant peculiarity though. In the isolated-wavepacket consideration, we assumed that the particle was at rest *before* the pulse arrives. However, for an infinite set of periodic sub-pulses, the particle can either appear suddenly in the already existing wave (like an electron under ionization), or a gradually increasing front of the beat wave runs up at the initially motionless particle (i.e., the amplitude a becomes a very slowly varying envelope).

In the first case, the particle motion strongly depends on the position of the particle's appearance. If the particle is placed in the beat-wave node, then every sub-pulse shifts the particle in the same manner as a single isolated wavepacket does. Figure 7a demonstrates this with numerical solutions of the equation of motion (1) for a simple particle in the field (18). However, if the particle is placed in an arbitrary position, it generally acquires a strong non-oscillatory velocity component, of the same order as the oscillatory one. The gradient

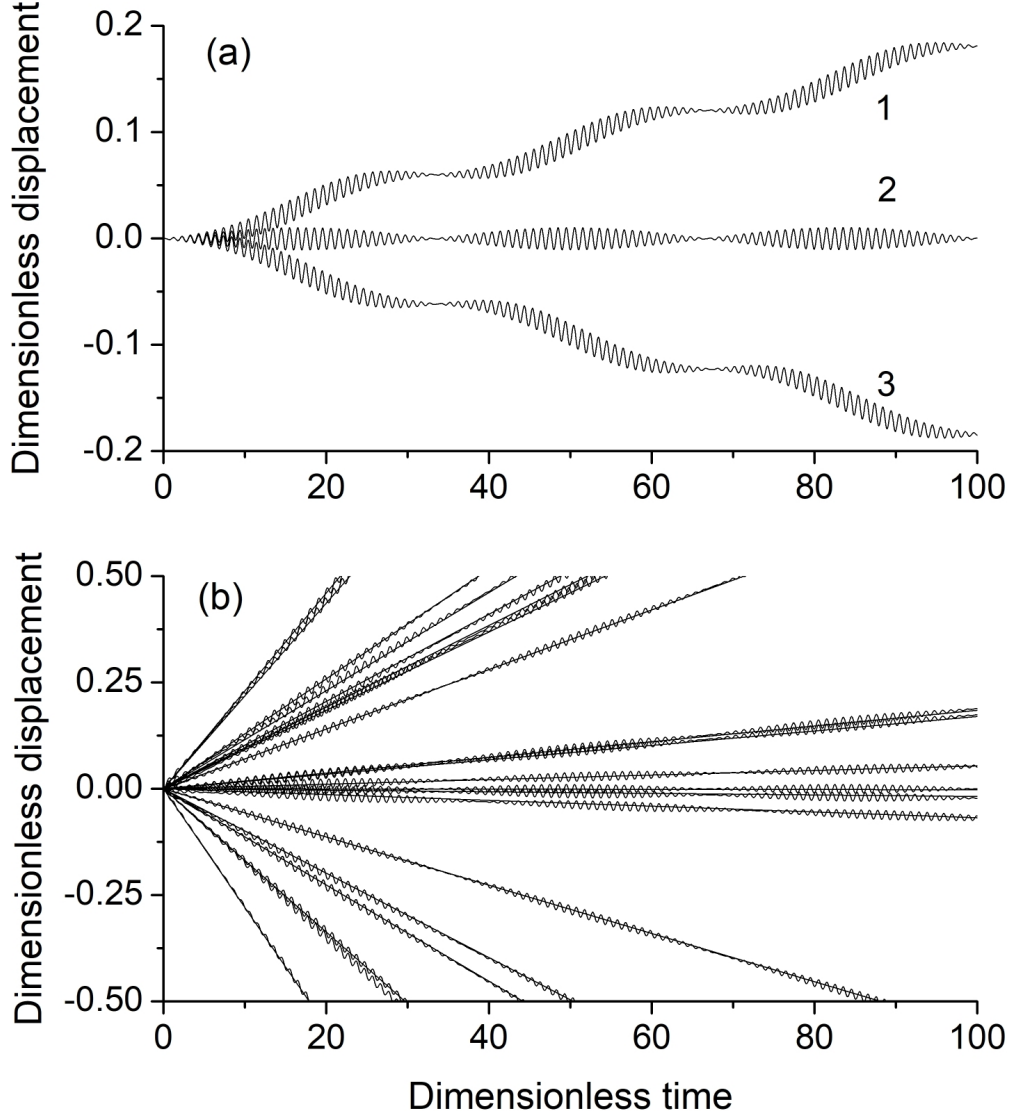


Figure 7. The particle motion in the beat wave field. The effective group velocity is negative, $u_g < 0$. (a) – the particle is placed in the beat wave node. 1 – the beat wave group velocity value $|u_g|$ is 10% larger than half of the phase velocity; 3 – the group velocity is 10% smaller than half of the phase velocity; 2 – the group velocity is equal to half of the phase velocity. (b) – The particles are initially randomly distributed along the wavelength near the beat wave node.

force is weak and is unable to change the direction of this steady motion of the particle. Figure 7b shows that the motion of such randomly placed particles depends only on the wave phase at the particle's appearance but not on the sub-pulse propagation direction.

A. Simple particle

We now consider the second case, where the beat wave amplitude is modulated as a ‘super-wavepacket’ of a finite length, see Fig. 6b. The forward front of such a wavepacket moves in the positive direction independently of the effective group velocity of the sub-pulses, u_g . This front can also be considered as a source of the ‘super-gradient’ force, different from the gradient forces at the sub-pulses.

Let us examine how these two types of forces influence the motion of a simple particle. The equation of motion has the same form as Eq. (1):

$$\frac{d^2\xi}{d\tau^2} = \mathcal{F}(\xi, \tau) \simeq A(\xi, \tau) \sin(\tau - \xi), \quad (19)$$

where $A(\xi, \tau) = a(\xi - \eta_g \tau) \cos(\Delta\nu\tau - \Delta\kappa\xi)$ and the envelope $a(\xi, \tau)$ is a ‘super-slow’ varying function. The time-averaged (over fast oscillations) equation of motions is obtained from Eq. (3):

$$\begin{aligned} \frac{d^2\bar{\xi}}{d\tau^2} &= -\frac{1}{2}A\left(\frac{\partial A}{\partial\xi} - 2\frac{\partial A}{\partial\tau}\right) \\ &= -\frac{1}{4}(1+2\eta_g)\frac{da^2}{d\theta} \cos^2(\Delta\nu\tau - \Delta\kappa\bar{\xi}) - \frac{1}{4}\Delta\kappa\left(1+2\frac{\Delta\nu}{\Delta\kappa}\right)a^2 \sin(2\Delta\nu\tau - 2\Delta\kappa\bar{\xi}). \end{aligned} \quad (20)$$

Let the characteristic spatial scale \mathcal{L} of the modulation $a(\xi - \eta_g \tau)$ satisfies $\Delta\kappa\mathcal{L} \gg 1$ and $\Delta\nu\mathcal{L}/\eta_g \gg 1$. Then, one can perform the second time averaging over oscillations with parameters $\Delta\kappa$ and $\Delta\nu$. In doing so, the displacement $\bar{\xi}$ is separated into the new ‘fast’ and ‘slow’ components, $\bar{\xi} = \tilde{\bar{\xi}} + \bar{\xi}$. Introducing variables $\tau' = 2|\Delta\nu|\tau$ and $\xi' = 2|\Delta\kappa|\bar{\xi}$, we rewrite Eq. (20) as follows:

$$\frac{d^2\xi'}{d\tau'^2} = -\frac{|\Delta\kappa|}{16\Delta\nu^2}(1+2\eta_g)\frac{da^2}{d\theta}[1+\cos(\tau' - s'\xi')] - \frac{s'\Delta\kappa^2}{8\Delta\nu^2}(1+2\Delta\nu/\Delta\kappa)a^2 \sin(\tau' - s'\xi'), \quad (21)$$

where $s' = \text{sgn}(u_g)$. The averaging of the first term on the right-hand side of Eq. (21) is obvious. The second term has the same form as the force \mathcal{F} in Eq. (1), and its contribution in the averaged equation of motion is described by Eq. (3), where the amplitude a is replaced by the coefficient at the sine function in Eq. (21). As a result, in the original variables, the averaged equation Eq. (21) becomes:

$$\frac{d^2\bar{\xi}}{d\tau^2} = -\frac{1}{8}\left[(1+2\eta_g) + \frac{(1+2s'|u_g|)^2}{16u_g^2}(1+2s'\eta_g/|u_g|)a^2\right]\frac{da^2}{d\theta}, \quad (22)$$

where $\theta = \bar{\xi} - \eta_g \tau$.

Since the particle velocity is small, one can approximate $\theta \simeq -\eta_g \tau$ and $d/d\theta \simeq -\eta_g^{-1} d/d\tau$ along the particle trajectory. Then, the particle's average velocity $\bar{u}_p = d\bar{\xi}/d\tau$ can be found by the integration of Eq. (22) with respect to τ :

$$\bar{u}_p = \frac{1}{8\eta_g} \left[(1 + 2\eta_g) + \frac{(1 + 2s'u_g)^2}{32u_g^2} \left(1 + 2s' \frac{\eta_g}{u_g} \right) a^2 \right] a^2. \quad (23)$$

Expression (23) shows that this velocity is always positive when $s' = 1$, and can be negative when $s' = -1$ and the wavepacket amplitude exceeds the critical value given by

$$a_{\text{crit}} = 4|u_g| \sqrt{\frac{2u_g(1 + 2\eta_g)}{(1 - 2u_g)^2(2\eta_g - u_g)}}. \quad (24)$$

This means that the modulated beat wave can provide controlled forward and backward transport of a simple particle. Within this simple general conclusion, the behavior of the particle exhibits a number of peculiarities.

Figure 8a shows the motion of a simple particle in the backward propagating ($s' = -1$) beat wave packets with different amplitudes. One can see that solutions of the original equation of motion (19) (black), the averaged equation (20) (gray), and the second-averaged equation (22) perfectly agree with each other. Note the increase of particle's velocity at the leading and trailing edges of the wavepacket when $a < a_{\text{crit}}$. The particle remains motionless ($\bar{u}_p = 0$) inside the wavepacket when $a = a_{\text{crit}}$.

If the amplitude a is so large that the particle's velocity is close to the sub-pulses group velocity $\bar{u}_p \simeq u_g$, the particle is trapped by the ponderomotive potential well between the sub-pulses. Then, it oscillates in this well, and moves with the well velocity u_g , whose value is independent of a , as shown in Fig. 8b. In the reference frame of the moving potential well, the potential magnitude is a slowly varying function of time. In the beginning, when the potential magnitude is small, the particle's motion is unbounded. When the potential magnitude becomes large enough, this motion is changed into localized oscillations in the potential well. In the rear end of the wavepacket, the particle is released from the potential well. Due to the adiabaticity of this process, the energy of the particle (in the potential-well frame) remains the same as it was before the wavepacket arrival. However, the particle can leave the potential well over its right or left barrier (in a random fashion). Correspondingly, the final particle's velocity can be equal to either u_g or $-u_g$, and in the laboratory reference frame, it becomes either $u_{p\text{fin}} = 0$ or $u_{p\text{fin}} = -2u_g$, as can be seen in Fig. 9.

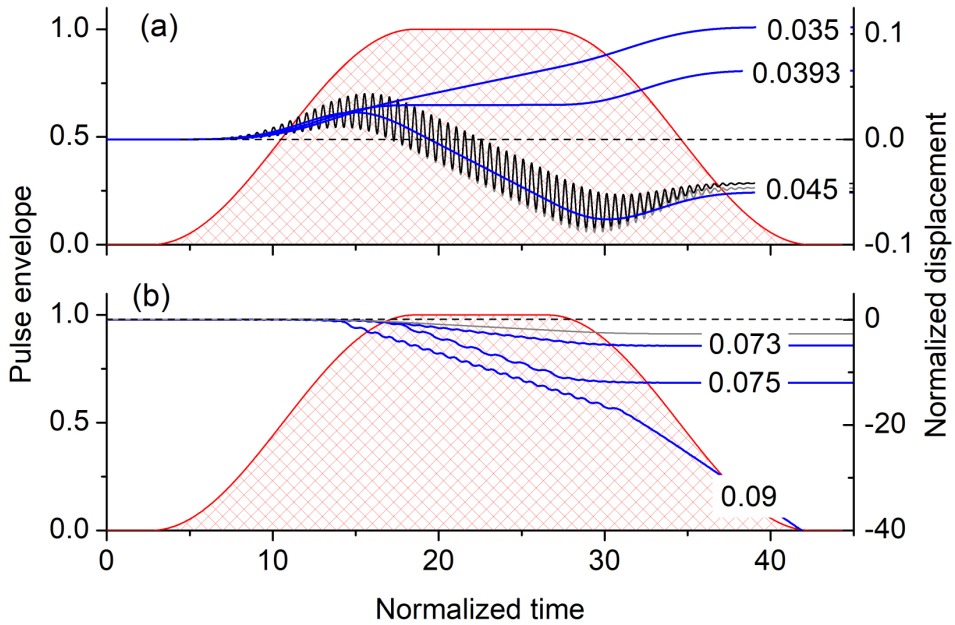


Figure 8. Trajectories of a simple particle in beat wave packets with $\eta_g = 0.9$, $|\Delta\nu| = 3 \cdot 10^{-4}$, $|\Delta\kappa| = 10^{-2}$, negative group velocity of sub-pulses, $s' = -1$, and different amplitudes. The pulse envelope is shown by the red patterned area. The amplitude value a_0 is shown near the corresponding curve. (a) $a_0 = 0.035$ – amplitude is smaller than the critical one. $a_0 = 0.0393$ – amplitude is equal to the critical one, the particle velocity is equal to zero in the interior of the pulse. $a_0 = 0.045$ – amplitude exceeds the critical value. Solutions of Eq. (19), and the averaged equation (20), are shown by practically indistinguishable oscillating black and gray lines. Solution of the twice-averaged Eq. (22) is shown by a smooth blue line. (b) $a_0 = 0.73$ – amplitude exceeds the critical value, but the particle is not trapped. The particle velocity is close to the group velocity of sub-pulses, and Eq. (22) loses its validity. $a_0 = 0.75$ and $a_0 = 0.09$ – particle is trapped by the ponderomotive potential well. The particle velocity in the pulse interior is equal to the sub-pulses group velocity u_g and is independent of the pulse amplitude.

To determine the amplitude a sufficient to trap the particle, let us write Eq. (21) in the reference frame of the ponderomotive potential well, using the substitution $\xi' = \xi'' + s'\tau'$ and $\theta = \xi - \eta_g\tau = [\xi'' - (\eta_g/u_g - s')] / 2|\Delta\kappa|$:

$$\frac{d^2\xi''}{d\tau'^2} = -\frac{1}{8u_g^2} \left[(1 + 2\eta_g) \frac{\partial a^2}{\partial \xi''} (1 + \cos \xi'') + (1 + 2s'|u_g|) a^2 \sin \xi'' \right]. \quad (25)$$

The two terms with sine and cosine functions in Eq. (25) can be combined in a single

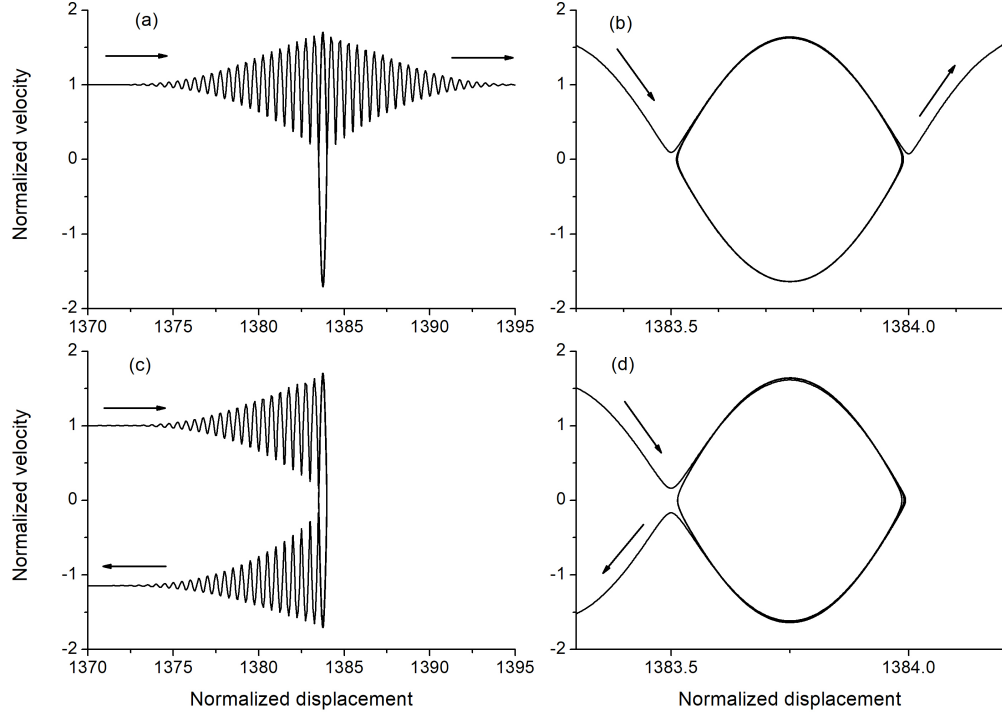


Figure 9. The particle's trajectory in the phase space in the frame of reference of the moving potential well. The particle is trapped by the potential well and leaves the well at the trailing edge of the pulse. (a) – The particle leaves the potential well over the right barrier; (b) – enlarged portion of phase space with the trajectory of the trapped particle. (c) and (d) – The same as in panels (a) and (b); the trapped particle leaves the potential well over the left barrier.

term $\propto \sin(\xi'' + \phi)$ with slowly varying phase $\phi \sim a^{-2}(\partial a^2 / \partial \xi'') \ll 1$. Neglecting this phase ϕ , i.e., neglecting the term with cosine, Eq. (25) can be written as:

$$\frac{d^2 \xi''}{d\tau'^2} = -\frac{\partial \mathcal{U}}{\partial \xi''}, \quad (26)$$

where

$$\mathcal{U} = \frac{a^2(\tau')}{8u_g^2} [(1 + 2\eta_g) + (1 + 2s'|u_g|) \cos \xi''] \quad (27)$$

is the ponderomotive potential of the beat wave. If the amplitude a is constant, then Eqs. (26) and (27) can be integrated:

$$u_p'' = \pm \sqrt{2[\mathcal{W} - \mathcal{U}(\xi'')]}, \quad (28)$$

where $u_p'' = d\xi''/d\tau'$ is the particle velocity, and \mathcal{W} is the constant kinetic energy of the particle. Equation (28) describes the particle trajectory $u_p''(\xi'')$ in the phase space (ξ'', u_p'') ,

even when the amplitude a varies slowly with time. To define the corresponding variation of the energy $\mathcal{W}(\tau')$, one can use the adiabatic invariant (the action) $\mathcal{I} = \int_0^{2\pi} u_p'' d\xi''$, whose value is defined by the initial state of the particle. If the particle was motionless before the pulse arrived, then $u_p''(0) = -s'$ in the chosen variables, $\mathcal{W}(0) = 1/2$, $\mathcal{U}(0) = 0$, and the initial action for a freely moving particle is $\mathcal{I} = -2s'\pi$. On the other hand, the action can be calculated via the integral

$$\begin{aligned} \mathcal{I} = -2s\pi &= -s' \int_0^{2\pi} d\xi'' \sqrt{2 \left[\mathcal{W} - \frac{(1+2\eta_g)a^2}{8u_g^2} - \frac{(1+2s'|u_g|)a^2}{8u_g^2} \cos \xi'' \right]} \\ &= 4\sqrt{2(\mathcal{W}' + \mathcal{U}')} \mathbf{E} \left(\sqrt{2\mathcal{U}' / (\mathcal{W}' + \mathcal{U}')} \right), \end{aligned} \quad (29)$$

where \mathbf{E} is the elliptic integral of the second kind, $\mathcal{W}' = \mathcal{W} - (1+2\eta_g)a^2/8u_g^2$, and $\mathcal{U}' = (1+2s'|u_g|)a^2/8u_g^2$. The particle is trapped when its trajectory reaches the separatrix, i.e., when $\mathcal{W}' = \mathcal{U}'$. Using Eq. (29), and taking into account that $\mathbf{E}(1) = 1$, this condition can be written as $\sqrt{\mathcal{U}'} = \pi/4$, which yields

$$a_{\text{trap}} = |u_g| \frac{\pi}{\sqrt{2(1+2s'|u_g|)}}. \quad (30)$$

Numerical solution of Eq. (19), presented in Fig. 8b, shows that the particle is trapped when the wavepacket amplitude $a > 0.074$. This result agrees well with Eq. (30) producing the value $a_{\text{trap}} \simeq 0.069$ for the parameters used in Fig. 8.

B. Polarizable particle

The motions of simple and polarizable particles differ little from each other. Indeed, Eq. (15) and Eq. (20) have similar structures, except for opposite signs in the right-hand side and the absence of the term $\propto \partial A / \partial \tau$ in Eq. (15). As a result, the time-averaged equation of motion for the polarizable particle takes the form:

$$\frac{d^2\bar{\xi}}{d\tau^2} = \frac{1}{2} \overline{A \frac{\partial A}{\partial \xi}} = \frac{1}{8} \frac{da^2}{d\theta} [(1 + \cos(2\Delta\nu\tau - 2\Delta\kappa\bar{\xi})) + \frac{1}{4} \Delta\kappa a^2 \sin(2\Delta\nu\tau - 2\Delta\kappa\bar{\xi})]. \quad (31)$$

Here, the polarizability coefficient α is eliminated by the amplitude re-normalization $a^2 \rightarrow \alpha a^2$.

Note that the replacements $(1+2\eta_g) \rightarrow -1$ and $(1+2s'|u_g|) \rightarrow -1$ transform Eq. (22) into Eq. (31). Therefore, the motion of a polarizable particle in a *forward*-propagating beat

wave ($s' = +1$) is entirely similar to the motion of a simple particle in the corresponding *backward-propagating* beat wave ($s' = -1$). This determines three regimes of the particle dynamics: negative shift after the super-wavepacket passage for $a < a_{\text{crit}}$, positive shift for $a > a_{\text{crit}}$, and trapping (with a positive shift) for $a > a_{\text{trap}} > a_{\text{crit}}$, where

$$a_{\text{crit}} = 4u_g \sqrt{\frac{2u_g}{u_g + 2\eta_g}}, \quad a_{\text{trap}} = u_g \frac{\pi}{\sqrt{2}}. \quad (32)$$

Figure 10 shows numerical calculations of a polarizable particle motion in a forward-propagating super-wavepacket of a beat wave, which agrees well with analytical predictions. For the beat wave pulse with the parameters specified above $a_{\text{crit}} = 0.0216$, and $a_{\text{tr}} = 0.067$, that agrees well with the results of numerical solutions of Eq. (31), presented in Fig. 10.

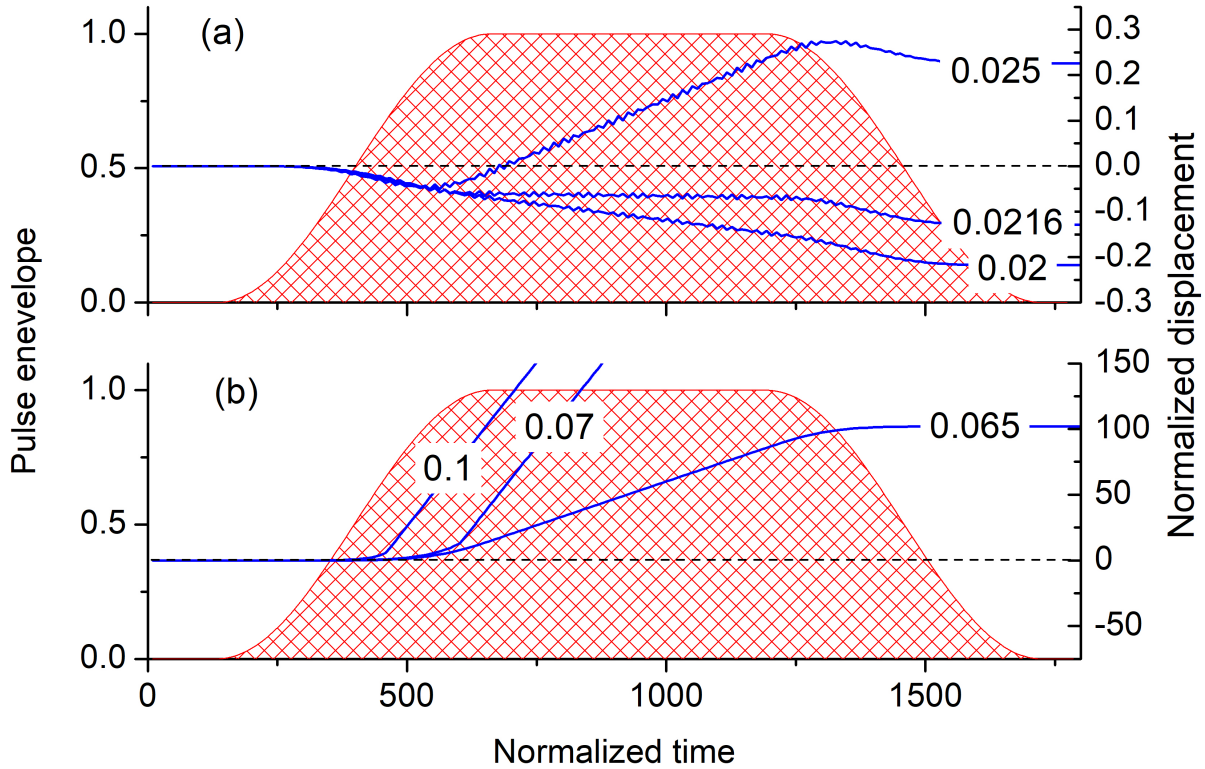


Figure 10. Numerical solutions of Eq. (15) providing exact trajectories of a polarizable particle in the beat-wave fields with various amplitudes and positive group velocity $s' = +1$ of the sub-pulses. The wavepacket parameters and notations are the same as in Fig. 8, which corresponds to $a_{\text{crit}} \simeq 0.0216$ and $a_{\text{trap}} \simeq 0.067$ in Eqs. (32).

C. Particles sorting

The motion of a simple particle in a backward-propagating beat wave, and the motion of a polarizable particle in a forward-propagating beat wave, demonstrate an unusual property: the direction of the particle shift can be easily controlled by the wave amplitude, see Figs. 8a and 10a. This property can be used for particle *sorting*, i.e., the separation of particles with different physical characteristics [8, 29, 30].

Since equations in this paper deal with the acceleration $d^2\xi/d\tau^2$, the field amplitude a is actually inversely proportional to the particle mass m . This means that amplitude-dependent behavior enables effective sorting by the particle density or size. Furthermore, the effective polarizability α of small optical or acoustic particles is also proportional to the particle's volume and depends on the material characteristics [8].

D. Comparison with previous works

Beat waves and analogous setups have been discussed and employed for manipulation of particles in different contexts. In particular, beat waves can be formed by the interference of two non-collinear plane waves or wave beams with slightly different frequencies. For example, a scheme using two non-collinear laser beams for the acceleration of electrons has been suggested in [31, 32] (see also [33]). However, these works considered only the acceleration of electrons; a backward-moving beat wave and pulling forces have not been studied.

The motion of dielectric particles in the field of two laser beams with *equal* frequencies but different longitudinal wavevector components was considered in [10, 29, 34]. Such field generates stationary spatially-periodic potential wells. Then, the phase shift between the beams can move the particles captured in the wells. Continuous motion of the trapped particle can be achieved by a continuous phase shift, i.e., a frequency shift [35].

V. CONCLUSIONS

We have described the dynamics of particles of various types in fast-oscillating fields of 1D quasi-monochromatic wavepackets and beat-wave packets. The ponderomotive force (which is sometimes referred to as the gradient force) depends to the same extent on slow spatial

and temporal variations of the wave amplitude. Our simplified models can be applied to charged particles ('simple particle'), anisotropic-shape particles ('dumbbell'), permanent-dipole particles, as well as polarizable particles ('induced dipole'). We paid particular attention to backward waves with oppositely-directed phase and group velocities, and to beat waves, in which the direction of the motion of sub-pulses can be controlled by the wave frequencies. Despite the simplicity of the 1D system under consideration, it exhibits a very rich behavior. We have provided a thorough theoretical analysis of various regimes of the particle dynamics, as well as numerical solutions of the equations of motion.

In particular, the motion of a simple point particle in a wavepacket field is conservative and depends on the forward or backward phase velocity of the wave. Next, dumbbell and permanent-dipole particles can demonstrate either regular or chaotic regimes depending on the wave amplitude. Finally, the dynamics of various particles in a beat wave crucially depends on the wave amplitude, and provides trapping in a moving potential well for high amplitudes.

Importantly, our models describe different mechanisms for the control of the particle motion from the wave source (pushing) or towards the source (pulling). In particular, small variations in the frequencies or amplitudes of interfering waves can readily alter the direction of the particle motion. We have found that the process of particle insertion in the beat wave field significantly affects its motion, but this difficulty can be overcome by using a 'super-wavepacket' with adiabatic modulation of the beat-wave amplitude.

ACKNOWLEDGMENTS

I am grateful to my colleague and son, Konstantin Bliokh, for his critical comments, which greatly improved the quality of the paper.

- [1] P. L. Kapitsa, Dynamic stability of a pendulum when its point of suspension vibrates, Sov. Phys. JETP **21**, 588 (1951).
- [2] A. V. Gaponov and M. A. Miller, Potential wells for charged particles in a high-frequency electromagnetic field, Zh. Eksp. Teor. Fiz. **34**, 242 (1958).

- [3] A. Ashkin, *Optical Trapping and Manipulation of Neutral Particles Using Lasers* (World Scientific, 2006).
- [4] D. G. Grier, A revolution in optical manipulation, *Nature* **424**, 810 (2003).
- [5] E. Esarey, C. B. Schroeder, and W. P. Leemans, Physics of laser-driven plasma-based electron accelerators, *Rev. Mod. Phys.* **81**, 1229 (2009).
- [6] A. Ozcelik, J. Rufo, F. Guo, Y. Gu, P. Li, J. Lata, and T. J. Huang, Acoustic tweezers for the life sciences, *Nat. Methods* **15**, 1021 (2018).
- [7] K. Dholakia, B. W. Drinkwater, and M. Ritsch-Marte, Comparing acoustic and optical forces for biomedical research, *Nat. Rev. Phys.* **2**, 480 (2020).
- [8] I. Toftul, S. Golat, F. J. Rodríguez-Fortuño, F. Nori, Y. Kivshar, and K. Y. Bliokh, Radiation forces and torques in optics and acoustics, *Rev. Mod. Phys.* <https://doi.org/10.1103/7zdw-p26g> (2026).
- [9] T. Tajima and J. Dawson, Laser electron accelerator, *Phys. Rev. Lett.* **43**, 267 (1979).
- [10] D. B. Ruffner and D. G. Grier, Optical Conveyors: A Class of Active Tractor Beams, *Phys. Rev. Lett.* **109**, 163903 (2012).
- [11] F. G. Mitri, Dynamic acoustic tractor beams, *J. Appl. Phys.* **117**, 094903 (2015).
- [12] S. Lepeshov and A. Krasnok, Virtual optical pulling force, *Optica* **7**, 1024 (2020).
- [13] K. Y. Bliokh, Y. P. Bliokh, and F. Nori, Ponderomotive forces, Stokes drift, and momentum in acoustic and electromagnetic waves, *Phys. Rev. A* **106**, L021503 (2022).
- [14] G. D. Bruce, P. Rodríguez-Sevilla, and K. Dholakia, Initiating revolutions for optical manipulation: the origins and applications of rotational dynamics of trapped particles, *Adv. Phys. X* **6**, 1838322 (2021).
- [15] J. F. Barry, D. J. McCarron, E. B. Norrgard, M. H. Steinecker, and D. DeMille, Magneto-optical trapping of a diatomic molecule, *Nature* **512**, 286 (2014).
- [16] C. Maher-McWilliams, P. Douglas, and P. Barker, Laser-driven acceleration of neutral particles, *Nat. Photonics* **6**, 386 (2012).
- [17] B. W. Drinkwater, A perspective on acoustical tweezers — devices, forces, and biomedical applications, *Appl. Phys. Lett.* **117**, 180501 (2020).
- [18] L. D. Landau and E. M. Lifshitz, *Mechanics* (Elsevier, 1982).
- [19] J. B. McLaughlin, Period-doubling bifurcations and chaotic motion for a parametrically forced pendulum, *J. Stat. Physics* **24**, 375 (1981).

- [20] W. van de Water, M. Hoppenbrouwers, and F. Christiansen, Unstable periodic orbits in the parametrically excited pendulum, *Phys. Rev. A* **44**, 6388 (1991).
- [21] G. B. Whitham, *Linear and Nonlinear Waves* (John Wiley & Sons, Inc., 1999).
- [22] J. Chen, J. Ng, Z. Lin, and C. T. Chan, Optical pulling force, *Nat. Photonics* **5**, 531 (2011).
- [23] A. Novitsky, C.-W. Qiu, and H. Wang, Single Gradientless Light Beam Drags Particles as Tractor Beams, *Phys. Rev. Lett.* **107**, 203601 (2011).
- [24] V. G. Veselago, The electrodynamics of substances with simultaneously negative values of ϵ and μ , *Sov. Phys. Usp.* **10**, 509 (1968).
- [25] D. R. Smith, W. J. Padilla, D. C. Vier, S. C. Nemat-Nasser, and S. Schultz, Composite medium with simultaneously negative permeability and permittivity, *Phys. Rev. Lett.* **84**, 4184 (2001).
- [26] J. S. Hummelt, X. Lu, H. Xu, I. Mastovsky, M. A. Shapiro, and R. J. Temkin, Coherent Cherenkov-Cyclotron Radiation Excited by an Electron Beam in a Metamaterial Waveguide, *Phys. Rev. Lett.* **117**, 237701 (2016).
- [27] P. J. B. Clarricoats and R. A. Waldron, Non-periodic slow-wave and backward-wave structures, *Journal of Electronics and Control* **8**, 455 (1960).
- [28] A. W. Trivelpiece, *Slow Wave Propagation in Plasma Waveguides* (San Francisco Press Inc., 1967).
- [29] O. Brzobohatý, V. Karásek, M. Šiler, L. Chvátal, T. Čižmár, and P. Zemánek, Experimental demonstration of optical transport, sorting and self-arrangement using a ‘tractor beam’, *Nat. Photonics* **7**, 123 (2013).
- [30] M. Yang, Y. Shi, Q. Song, Z. Wei, X. Dun, Z. Wang, Z. Wang, C.-W. Qiu, H. Zhang, and X. Cheng, Optical sorting: past, present and future, *Light Sci. Appl.* **14**, 103 (2025).
- [31] K. Sakai, Particle trapping and acceleration by beats of two laser beams in vacuum, *J. Phys. Soc. Jpn.* **58**, 2325 (1989).
- [32] K. Sakai, M. Ogiwara, S. Takeuchi, and M. Matsumoto, Electron acceleration by beat wave of two gaussian laser beams in vacuum, *Jap. J. Appl. Phys.* **30**, L374 (1991).
- [33] B. Hafizi, A. Ting, E. Esarey, P. Sprangle, and J. Krall, Vacuum beat wave acceleration, *Phys. Rev. E* **55**, 5924 (1997).
- [34] T. Čižmár, V. Kollárová, Z. Bouchal, and P. Zemánek, Sub-micron particle organization by self-imaging of non-diffracting beams’, *New J. of Phys.* **8**, 43 (2006).

[35] M. Sadgrove, S. Wimberger, and S. Chormaic, Quantum coherent tractor beam effect for atoms trapped near a nanowaveguide, *Sci. Rep.* **6**, 28905 (2016).